Advances in friction stir welding of steel – project HILDA

Athanasios Toumpis[a,*], Alexander Galloway[a], Stephen Cater[b], Daniel Micallef[c], Duncan Camilleri[c], Nicolas Poletz[d], Larbi Arbaoui[d]

[a]University of Strathclyde, Glasgow, United Kingdom
[b]TWI Technology Centre (Yorkshire), Rotherham, United Kingdom
[c]University of Malta, Msida, Malta
[d]Cenaero, Gosselies, Belgium

Abstract

Friction stir welding (FSW) of steel is an advanced joining process which is expected to deliver considerable technical and commercial benefits to the European waterborne manufacturing sector. A microstructure and property evaluation of friction stir welded DH36 6mm plate has been undertaken. The study examined a wide range of process parameters and, from this, a process parameter envelope has been developed and an initial process parameter set established that gives good welding properties. Thermo-mechanical deformation studies were developed to generate flow stress regimes over a range of stain rates and temperatures and these data will support the on-going local numerical modelling development. A preliminary thermo-fluid model has been developed to predict temperature and material flow during the FSW of steel grade DH36. In parallel, a global numerical model is being developed to predict the inherent residual stresses and distortion of FSW butt welded assemblies often in excess of 6m long plate.

Keywords: Friction stir welding; Tensile testing; Low alloy steel; Flow stress; Thermo-fluid model; Eulerian formulation; Friction condition; Numerical techniques; Thermo-elastoplastic models.

Résumé

Le soudage par friction-malaxage de l'acier est un procédé d'assemblage avancée qui offre des avantages techniques et commerciaux considérables au secteur Européen de la construction navale. Une évaluation de la microstructure et propriétés d'une plaque DH36 soudée par friction-malaxage a été réalisée. L'étude a examiné une large gamme de paramètres de procédé et, à partir de cela, une enveloppe de paramètres de procédé a été développée et un ensemble de paramètres initial, qui donne des bonnes propriétés de soudage, a été mis au point. Des études de déformation thermo-mécaniques ont été réalisées pour produire des régimes de débit stress sur une gamme des vitesses de déformation et températures, et ces données vont contribuer au développement courant des modèles numériques locaux. Une modèle thermo-fluide préliminaire a été mise au point pour prédire le flux de température et matériel pendant le soudage par friction-malaxage d'acier DH36. Parallèlement, une modèle globale numérique a été développée pour prédire les tensions et distorsions inhérentes des assemblages soudées par friction-malaxage en plaques qui excèdent souvent une longueur de 6 m.

Mots-clé: Soudage par friction-malaxage; Essais de résistance à la traction; Faibles en acier allié; Débit stress; Modèle thermo-fluide; Formulation eulérien; Condition de friction; Techniques numériques; Modèles thermo-élasto-plastiques.

* Tel.: +44-(0)7513-621-906.
E-mail address: athanasios.toumpis@strath.ac.uk.

Nomenclature

α	friction coefficient	q_{fr}	friction heat flux	$\dot{\varepsilon}$	deviatoric strain rate
σ	stress tensor	n	velocity sensitivity	Q_p	heat input by tool pin [W]
v	velocity	ρ	density	R_s	tool shoulder radius [m]
K	consistency	c_p	specific heat capacity	R_p	tool pin radius [m]
λ	thermal conductivity	h	tool height [m]	Q_s	heat input by tool shoulder [W]
M	strain rate sensitivity	υ	Taylor Quiney	q"	heat flux from tool shoulder [W/m^2]
vg	sliding velocity	q'''	volumetric heat generation from tool pin [W/m^3]		
r	relative position from tool centre [m]				

1. Introduction

Friction stir welding (FSW) is a solid state joining process during which a constantly rotating, cylindrical-shouldered tool with a profiled probe is traversed at a constant rate along the joint between two clamped pieces of butted material. The probe is slightly shorter than the weld depth required, with the tool shoulder riding along the top of the work piece surface. The material is thermo-mechanically worked and heated high enough for plastic deformation to occur but never molten. This heat, along with that generated by the mechanical mixing process and the adiabatic shearing within the material, causes the stirred materials to soften. As the tool is moved forward a special profile on the probe forces plasticised material to the rear where clamping force assists in a forged consolidation of the weld.

The University of Strathclyde is coordinating project HILDA (High Integrity Low Distortion Assembly) which is supported from an FP7 budget of €2.1 million. Its main focus is on FSW of steel grade DH36, a low alloy steel utilised in the European shipbuilding industry. For FSW of steel to become economically and technically viable for introduction in the shipbuilding industry, it should evolve into a process competitive with conventional fusion welding methods. In the shipbuilding sector, this requirement is translated into high speed welds (in millimetres per minute) of acceptable quality. Therefore, an optimisation study is a fundamental step towards this direction; that is, a study concerned with establishing the limits of the process (the process envelope) in terms of the two more significant parameters which can be directly controlled, tool traverse speed and tool rotational speed.

FSW of steel is expected to deliver substantial commercial and technical benefits to the European waterborne manufacturing sector such as reduced pre-weld preparation and re-work, manpower savings, scope for redesign of assembly lines, and low distortion, high quality welds of excellent fatigue properties. In one example from FSW of aluminium, Norwegian shipyard Fjellstrand reported that "using prefabricated FSW panels has enabled a 40% increase in production capacity and turn-over at the yard". Issues associated with setup, fixture and tooling costs along with reduced health and safety, training, consumable and material usage costs compared to conventional fusion welding techniques should also influence the introduction of this innovative welding process in industry. There are a number of currently identified obstacles, deeper scientific understanding of the process on steel, engagement with the shipbuilding industry, use of fillet welds, different thicknesses and joint design, which will be required to overcome before full acceptance of the process is achieved.

2. Development of process parameter envelope

Seventy friction stir welds in 6 mm thick DH36 steel, each up to 2 m in length, have been made to date using the PowerStir FSW machine with a hybrid WRe-pcBN tool. Initial work was conducted with the tool rotating at 200rpm and traversing at 100mm/min, and the process evolved from there. In simplistic terms, the tool rotation rate controls the frictional heat input to the weld zone and plasticises the steel whilst the traverse rate of the tool influences the weld quench and has a significant effect upon the microstructures obtained. It is desirable to use process parameters that produce the best weld in terms of microstructure and mechanical properties, the current tool technology for steel FSW is still relatively immature and attention must be paid to ensuring that the welding environment is not so aggressive that the tool's life is shortened by the welding process. A compromise must therefore be made between selecting parameters that give good weld properties and parameters that extend the life of the tool and thereby improve the economic viability of the FSW process in steel. A number of welds were initially made using the previously stated process parameters as this provided a baseline data set of the generated

forces, torques and heat inputs resulting from these parameters. These data provided the basis for expanding the process envelope to higher welding speeds.

FSW needs to be competitive to conventional fusion welding techniques in terms of welding speed, and thus the process parameters were then shifted to explore higher welding speeds. If the tool is to be traversed through the steel being welded more quickly, then it is necessary to ensure that the steel ahead of the tool is sufficiently plasticised to ensure that the forces experienced by the tool do not increase to the point where the tool fails, and the steel continues to flow around the tool and can be consolidated behind it effectively. To weld at higher travel speeds, it is necessary to increase the tool rotation rate. Parameter selection is therefore a complex process with many interdependent variables, many of which are currently poorly understood.

Once a baseline understanding of the welding process was achieved, the primary process parameters of tool rotation rate and tool traverse rate were increased. The objective was to increase the welding travel speed from 100 mm/min to 350 mm/min, the point at which FSW would become competitive with fusion welding process in terms of production speed of acceptable quality. However, the parameter envelope was further extended to produce faster than anticipated welding speeds and this highly novel approach has resulted in a step change in the potential competitiveness of FSW for steel. In summary the welding speeds were segregated into three categories; Slow (200 rpm with traverse speeds of 100 – 200 mm/min), Intermediate (400-450rpm with traverse speeds of 250-400 mm/min), and Fast (600-700rpm with traverse speeds of 500mm/min). The purpose of the present study is to assess the impact of this increase on the properties and quality of the weld deposit.

3. Microstructure evaluation

Microstructural characterisation is the first experimental step towards establishing the limits of the FSW process. It is a fundamental stage as, through its relationship to predicting the mechanical properties of the weld, an understanding of the microstructure develops important information regarding the properties that are likely to be attained in the weld zone. A secondary outcome of the microstructural assessment is to provide information related to undesirable process induced defects or flaws that could compromise the integrity of the weld, the absence of which provides reassurance that the weld process parameters reported will lead to an acceptable level of quality. A summary of these features are reported herein.

One sample was transversely sectioned from a random position within the steady state condition region of each of the nineteen welds. In the steady state region, the forces that the FSW tool sustains stabilise, the weld quality is improved, and any sample removed from any position within the steady state region is expected to be representative of the properties of the entire weld. The region of steady state condition is commonly identified by visual observation of the welded plates (a good quality surface without excessive flash formation, voids or cracks), and confirmed by analysis of the forces (on the longitudinal and vertical direction) on the tool; this is typically established beyond the first 150 mm of welding.

Macrographic examination is widely used as the first stage of the microstructural characterisation process as it can often highlight regions of interest that require more detailed examination within the weld region. In such cases, more detailed examination was performed with the aid of a light optical microscope that involved taking several micrographic images from each sample being studied. The following nomenclature is adopted in the present study and the main regions of the weld zone are illustrated in Figure 1, where:

- AD: Advancing side, the side where the rotating FSW tool pushes the metal towards the weld direction, i.e. forwards. The convention employed for the entire project is that samples are prepared so that the advancing side is presented on the left side of all images.
- RT: Retreating side, the side where the rotating tool pushes the metal in a direction opposite to the weld direction, i.e. backwards.
- TMAZ: Thermo-mechanically affected zone in which the material has been thermo-mechanically stirred.
- Weld root: part of TMAZ, around and below the tip of the FSW tool's pin.
- HAZ: Heat affected zone, where the metal has been affected by heat but not mechanically stirred.
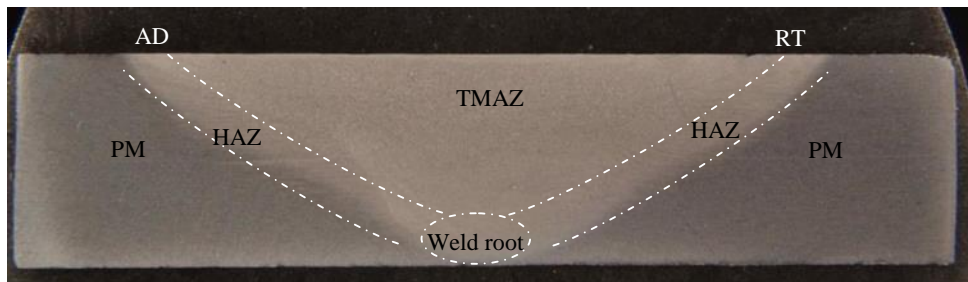- PM: Parent material, metal not affected by the process.

Fig. 1. A typical macrograph of the friction stir weld region

The group of slow welds presented a very homogeneous microstructure without any flaws. These exhibited a ferrite rich microstructure with highly refined grains of random geometry. A very small content of acicular-shaped bainitic ferrite was in one of the slow speed welds (Figure 2a), the content of which was seen to steadily increase with increasing traverse speed and constant rotational speed (200 rpm). This observation suggests that the cooling rate is increasing with increasing traverse speed. Additionally, there appears to be a threshold value of approximately 130 mm/min above which acicular-shaped bainitic ferrite appears at a small ratio relative to the above described ferrite rich microstructure.
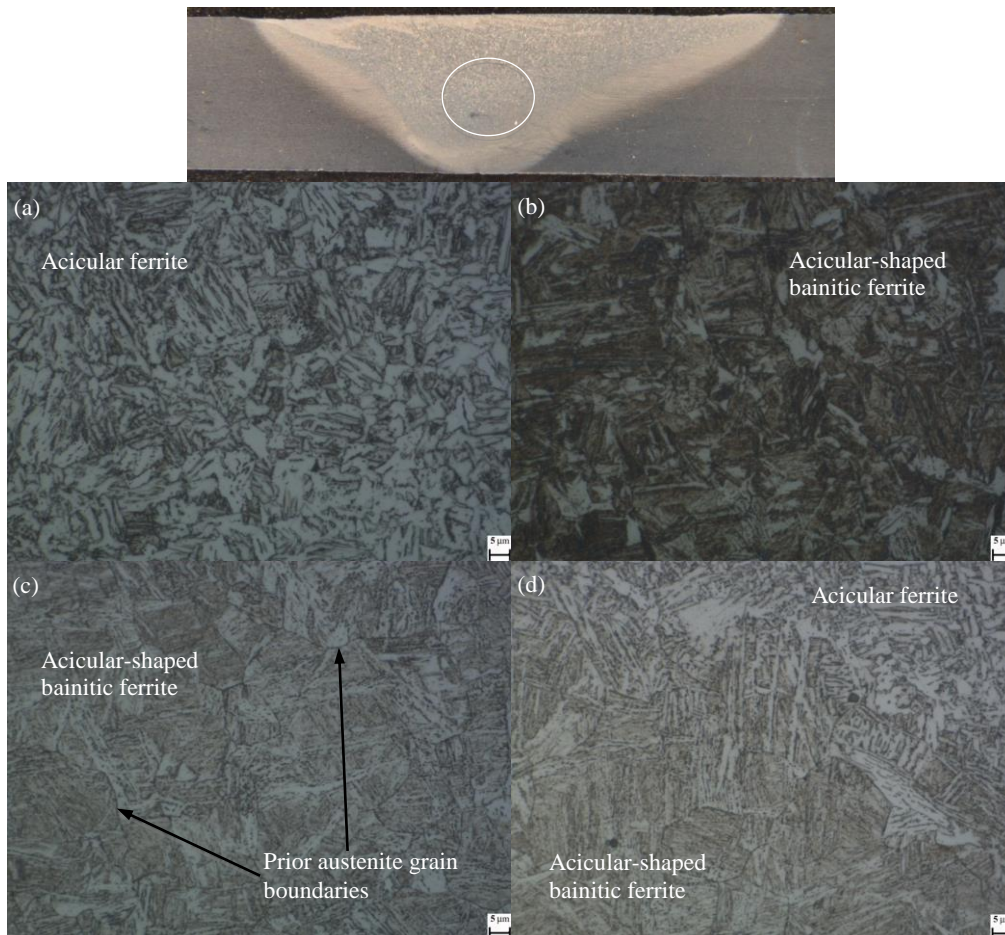

Fig. 2. Microstructure of mid-TMAZ [x1000, Etched] (a) Slow; (b) Intermediate 1; (c) Intermediate 2; (d) Fast

In the intermediate group of welds with rotational speed of 400 rpm and as traverse speed is seen to increase, the microstructure becomes more heterogeneous, with regions of increasing bainite content (suggesting an increased cooling rate). However, this heterogeneous microstructure does not seem to have a significant effect on the mechanical properties (see section 4). Still, one intermediate weld is very homogeneous, with an acicular-shaped

bainitic ferrite microstructure (Figure 2b); this would suggest that a good balance of rotational and traverse speed has been achieved. Overall, the FSW process appears to be tolerant to welding speed variations at the 450 rpm rotational speed. Both welds in this intermediate group exhibit a homogeneous, fully acicular-shaped bainitic ferrite microstructure with prior austenite grain boundaries as shown in Figure 2c.

At the fast welding speed of 500 mm/min, the microstructure of all five welds becomes very heterogeneous, with poorly mixed regions of acicular ferrite and varying bainite content. The presence of bainite has increased considerably in this group due to the even higher cooling rate that it is expected to occur. Prior austenite grain boundaries are easily detected on the regions of bainite predominant microstructure. Two distinct microstructures co-exist within the TMAZ of one of the fast welds (Figure 2d); these would be expected to act as stress concentration regions. Yet, this weld's parameters seem to have achieved a good balance of traverse and rotational speed that is translated into satisfactory tensile behaviour. This could be attributed to the grain refinement and a suitable ratio of microstructures overtaking the negative effects of heterogeneity.

It is worthy of note that at faster welding speeds the process becomes very sensitive to parameters change, i.e. variations in rotational speed in this group of welds. However, no voids or cracks or others flaws are detected in the bulk of the weld zone (TMAZ), and especially in the top advancing side where the shear forces on the metal are expected to be the highest. Hence, high speed FSW of steel grade DH36 is feasible; the process is tolerant to parameter variation in low and intermediate speeds but less tolerant at the highest speed (500 mm/min).

4. Mechanical property assessment

Sixty transverse tensile tests (extracted from the slow, intermediate and fast weld speeds) were performed on an Instron 8802 servo-hydraulic uniaxial tensile testing system in accordance with ISO Standards. The following general results were observed:

- All slow and intermediate weld samples failed in the parent material in a typical ductile fracture. This suggests that these fifteen sets of weld parameters produced welds of higher strength than the parent material.
- Four out of the five fast welds failed in the outer boundary of the advancing side of the weld zone in a brittle manner. This fracture region appears to correspond to the top AD TMAZ region where non-metallic inclusions were found to be interconnected in an incomplete fusion characteristic (i.e. cracks).
- One of the fast welds failed in the parent material although exhibiting a very heterogeneous microstructure with possible stress concentration regions. It would appear that this set of parameters achieves a good balance of rotational speed (sufficient heat input for proper thermo-mechanical stirring) and traverse speed (affecting the cooling rate which governs the ratio of phases) to produce acceptable quality welds.

5. Thermo-mechanical deformation

The behaviour of a metal under thermo-mechanical deformation can be accurately represented by determining the evolution of flow stress as a function of test temperature and strain rate (Nowotnik, 2008). The flow stress of a material, the stress that yields the material as a function of strain, is an important consideration when deciding on the basic parameters of a metalworking process (Boisse et al., 2003, Dieter et al., 2003). It is influenced by many factors; material properties such as grain size, crystal structure, existing phases, and process requirements including temperature and strain rate (Nowotnik, 2008, Dieter et al., 2003). Hence, as the FSW process is developed by thermo-mechanical stirring, it is critical that an understanding of the flow stress generated over a range of temperatures and strain rates is achieved such that improvements in the accuracy of any predictive modelling being undertaken takes account of these experimental data.

For example, Cenaero is building a local microstructural numerical model which takes into account the deformation of the metal only a few millimetres around the pin of the FSW tool that has been plunged in between the two plates to be welded. This model assumes the material follows rigid visco-plastic behaviour during FSW; in these conditions of high temperature and strain rate that prevail under the shoulder and around the pin of the tool, only the plastic region of the deformation is used as the elastic region is considered negligible in comparison. As a consequence, it was deemed necessary to determine the evolution of viscosity with respect to temperature and strain rate. Therefore, establishing the flow stress of the material under examination has been

one of the fundamental elements supporting the local model. There is very limited data available in the relevant technical literature, none of which is on steel grade DH36. Hence, the following study was deemed necessary.

An extensive flow stress testing programme has been conducted during which fifty-four uniaxial hot compression tests have been performed using the Gleeble 3800 thermo-mechanical testing apparatus. The testing programme has been implemented according to the guidelines set by Roebuck et al. (2006). The deformation parameters were derived from a preliminary analysis of data generated by thermocouples fitted inside plates during welding by TWI, and in collaboration with Cenaero. Material flow occurring below 700°C and with low strain rate is expected to be relatively insignificant. Conversely, the metal under the shoulder and around the pin of the tool is experiencing temperatures close or above 1000°C and high strain rates (10/s – 100/s).

5.1. Summary of data generated

The evolution of the flow stress followed two patterns (Nowotnik, 2008, Dieter et al., 2003), and these were verified in DH36. First, the flow stress is seen to increase with increasing strain rate. This is represented in Figure 3 where the flow stress curves of four sets of tests with increasing strain rate and constant temperature have been superimposed. Second, the flow stress is seen to decrease with increasing temperature; this relation was also confirmed by our experimental data.
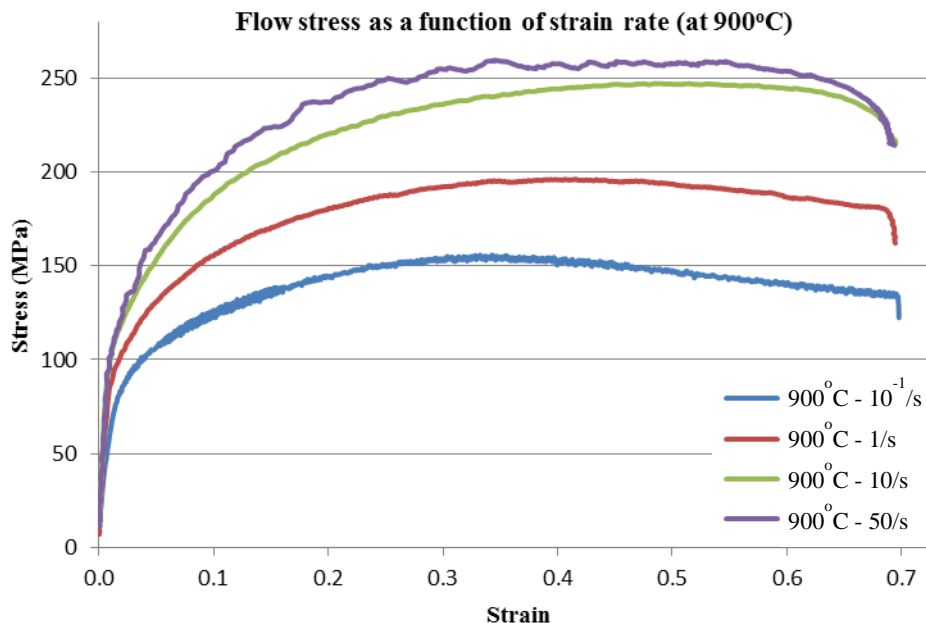

Fig. 3. Evolution of flow stress with increasing strain rate.

6. Global numerical modelling

FSW involves a highly multi-physics joining fabrication procedure. In order to fully capture and accurately predict the inherent residual stresses and distortion the fluid, thermal, metallurgical and elasto-plastic constitutive laws have to interact together in a coupled fashion. The HILDA project is thus developing robust numerical procedures that are able to capture the local and global influence of FSW of typical butt-welded assemblies. Various simplifications are possible. In the first instance the multi-physics problem is divided into a number of systems that are solved independently but interact together through an exchange of results. For instance the fluid, thermal and metallurgical solutions are solved independently by means of an intensive computational model through a so called 'local' model, the outcomes of which are then fed into a thermo-elasto-plastic global model.

The thermo-elasto-plastic solution is further fragmented by uncoupling the thermal and structural aspects. Firstly a thermal model is considered to predict the global far-field thermal gradients developed during FSW. The predicted heat generated due to FSW from the local model is fed into this global thermal model as boundary

conditions and any influences due to heat sinks developed due to global clamping and plate to machine bed backing are also included. The thermal gradients predicted by this model are then fed into an elasto-plastic structural model as thermal strains. The solution obtained by the structural model is highly dependent on the correct application of material properties and hence the predicted metallurgical transformations defined in the local model together with an experimental regime, are also fed into this global model. The influence of clamping and restraints developed during the process are also considered at this stage.

Though the global model explained above uncouples the thermal and structural systems the transient nature of the process still requires significant computational time to predict the final residual stresses and distortion in 6m long plates. Further simplifications are required to reduce the computational time of current models that can take up to a week to solve to a relatively small amount of time and power without compromising the integrity and prediction of residual stresses and distortion. In essence the global model will also consider reducing the solution from a transient structural analysis to a static heating, cooling and unclamping three-step solution following the basis given by Camilleri et al. (2005). To maintain confidence in the developed global numerical models a rigorous experimental test procedure will be undertaken.

6.1. Thermal numerical models and experimental validation

The heat generated due to FSW is assumed to arise from friction developed at the tool shoulder and pin together with plastic heat generation due to the stirring of metal. The heat developed is modelled by means of two heat generation parameters that include a heat flux at the tool shoulder-plate interface following the linear variation given in equation 1 and a volumetric heat input at pin tip and sides following equation 2. These equations form the basis of the heat flux predicted by the local model but require further validation and refinement. Nonetheless at this stage these assumptions have provided significantly good comparison with the experimental test results. Figure 4 shows a comparison between the maximum temperature measured at various salient points in weld zone with the predicted temperatures using such heat flux and heat generation models.

$$q'' = 3Q_s r/[\ 2\pi(R_s^3 - R_p^3)] \tag{1}$$
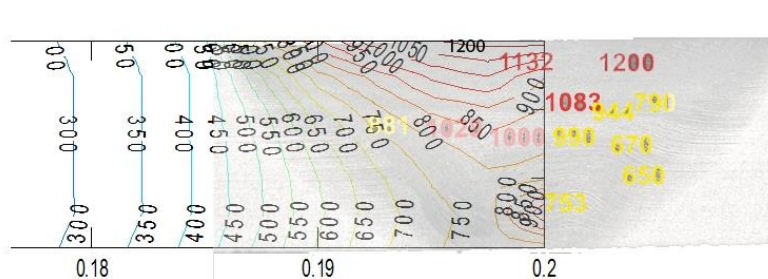
$$q''' = Q_p/\ \pi R_p^2 h \tag{2}$$

Fig. 4. Comparison between experimental and numerical maximum temperature measured and predicted at salient points within the weld region (experimental measurements - colour, numerical prediction - contour lines).

Though at this stage a relatively crude model is assumed for the heat input it was found that the temperatures developed in the thermal model are highly influenced by heat sinks present at the welding configuration adopted. A relatively large amount of heat proportion developed at the weld is being extracted due to heat sink. Various heat sink models were considered that were found to have a significant influence on the near and, most importantly for the global models, on the far-field temperatures. The amount of heat extraction is highly dependent on the material used as a backing strip and the thermal contact developed between the plate and the machine bed. For instance, temperatures in the region of 500ºC have been recorded at the backing strip suggesting full thermal contact.

6.2. Current and on-going structural numerical modelling and validation

Temperature dependant material properties have been assumed, however these properties have been extracted from previous projects dealing with fusion welding where heating and cooling rates are significantly different. In particular the primary driving force leading to residual stresses and distortion are a result of the thermal strains

developed that are in turn a function of the expansivity including any volumetric changes due to phase transformations. The influence of clamping and other restraints have also been considered in current models. Again the restraint offered by the clamps can have a significant influence on the final residual stresses and ultimately distortion. Figure 5 shows the predicted residual stresses using a transient elasto-plastic model for a 0.5 m long plate with clamping still being applied. The influence of clamping is being further investigated by means of strain gauges. At this stage the predicted distortion is substantially low.
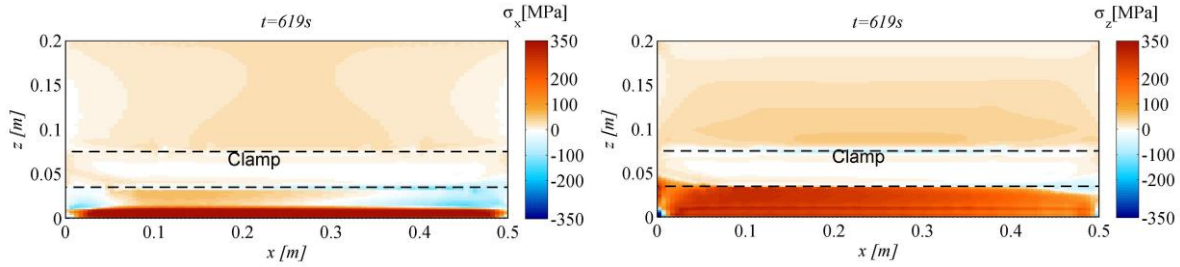

Fig. 5. Predicted residual stresses using current global model (a) Longitudinal residual stresses; (b) Transverse residual stresses (Micallef et al., 2013).

7. Thermo-fluid model for numerical simulation of DH36 steel assembly by FSW

7.1. Computational domain and mesh

An Eulerian finite element model developed in Morfeo software is used to compute thermal and material flow. The finite element model is focused on a region located around the tool (Figure 6). The computational domain Ω is composed of three main connected subdomains: tool, workpiece and backing plate. The finite element mesh is fixed in space and time while material flows through it. The mesh is refined at the tool/workpiece interface $\partial\Omega_C$ and in the stirred zone in order to capture high temperature and velocity gradients in this area.
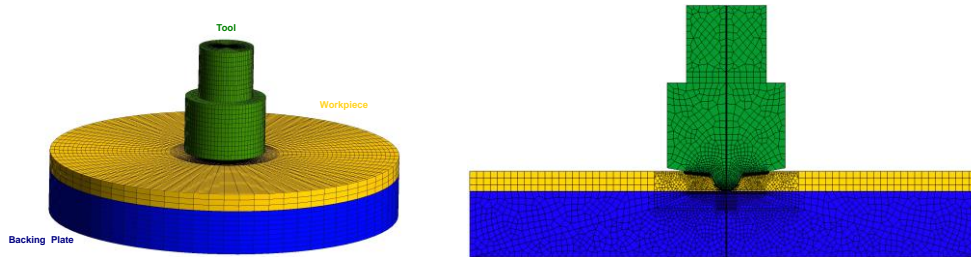

Fig. 6. (a) 3D mesh model; (b) cross section of the mesh centred on stirred zone and tool/workpiece interface.

7.2. Mechanical equations and constitutive equations: material behaviour

For FSW of stainless steel, the Reynolds number value for FSW of steel is around 5×10^{-6}. The inertial term is neglected compared to viscous term. The gravity force is also assumed to be small compared to other force (viscous stress). The momentum conservation equation is simplified as:

$$\nabla\sigma = 0 \ on \ \Omega \tag{3}$$

The density variation with space and time of the considered material is neglected. The material is then considered as incompressible (equations 3 and 4 are discretized using a mixed velocity/pressure formulation):

$$\nabla v = 0 \ on \ \Omega \tag{4}$$

The FSW process involves very large strain and strain rate, the elastic strain can be neglected compared to plastic strain. For this case, the rigid-viscoplastic approximation can be considered. In the thermo-fluid model, the expression used for the deviatoric part of the stress tensor is based on the Norton-Hoff law (5). In this law, the stress is expressed as a power law of the deviatoric strain rate with two thermo-dependent parameters.

$$\sigma = 2\, K(T)\, (\sqrt{3}\, \dot{\varepsilon}_{eq})^{m(T)-1}\, \dot{\varepsilon} + pI \qquad (5)$$

7.3. Friction and contact conditions

The relative velocity between the tool and the workpiece is modelled by a contact condition with friction. The sliding velocity (tangential part of the relative velocity) at the tool/workpiece interface is computed as follows:

$$v_g = v_{tool}(X) - v - (v_{tool}(X) - v).n \quad on\ \partial\Omega_C \qquad (6)$$

A non-penetration condition is imposed at this interface using kinematic constraint. The frictional resistance to the relative motion between the two bodies is defined by the tangential stress vector. The Norton friction law is considered to express the tangential stress vector:

$$\Gamma = \alpha K(T)\, |v_g|^{n-1} v_g \quad on\ \partial\Omega_C \qquad (7)$$

7.4. Thermal equations

The energy equation is solved to determine the temperature distribution in the three subdomains:

$$\rho c_p v\, \nabla T = \nabla(\lambda\, \nabla T) + \upsilon\, 2\, K(T)\, (\sqrt{3}\, \dot{\varepsilon}_{eq})^{m(T)-1}\, \dot{\varepsilon}:\dot{\varepsilon} \quad on\ \Omega \qquad (8)$$

A source term is introduced in equation 8 to take into account the viscous dissipation contribution to the total energy balance. Relative motion induces energy generation at the interface. The generated heat flux based on Norton friction law is expressed as:

$$q_{fr} = \alpha K(T)|v_g|^{n+1} \quad on\ \partial\Omega_C \qquad (9)$$

7.5. Experimental characterization of DH36 viscosity

In order to simulate the friction stir welding of DH36 steel plates, the thermo-mechanical behaviour of the material is required. Experimental measurements based on Gleeble tests have provided flow stress data in large range of strain rate and temperature. Norton-Hoff law parameters in function of temperature are obtained by inverse analysis from experimental flow stress data for temperature range between 700°C and 1100°C.

7.6. Numerical sensitivity analysis

A sensitivity study on the tool penetration depth was conducted. It appears that a slight diminution of the penetration depth may strongly affect the resulting temperature distribution. By decreasing this penetration with a same value of friction coefficient, the numerical tool velocity magnitude will decrease as well as the computed temperature in plates. Temperature distribution obtained in Figure 7a shows good trends with respect to preliminary experimental results especially in terms of HAZ extension with respect to the shoulder contact area.
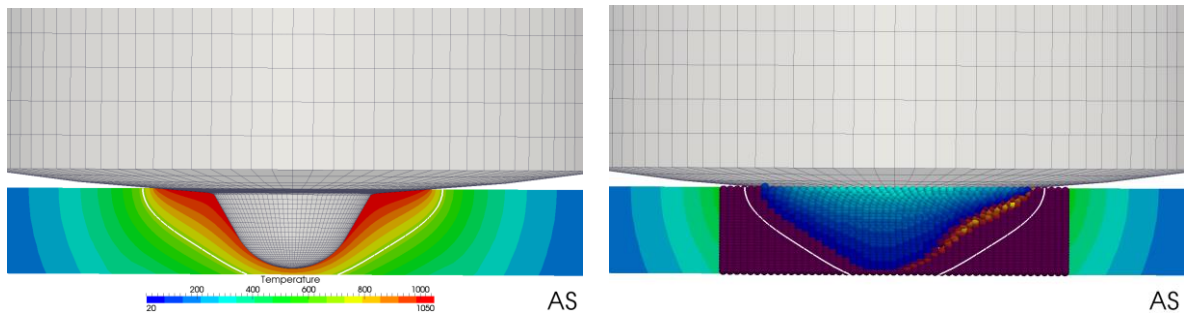

Fig. 7. (a) 3D mesh model; (b) cross section of the mesh centred on stirred zone and tool/workpiece interface.

The thermo-mechanically affected zone for the same tool depth penetration is presented in Figure 7b. The white line represents an estimate of the HAZ (700°C iso value). The blue and red particles in the centre correspond to the deformed region in the welded plate. The extension of the TMAZ is clearly not symmetric with respect to the

tool axis. The shape of the TMAZ on the retreating side and advancing side seems to be in good agreement with first experimental results.

8. Conclusions

* The welding (traverse) speed has been increased substantially compared to almost a year ago. This represents considerable potential economic advantages in terms of the competitiveness of FSW to conventional fusion welding processes.
* An initial understanding of the relationship between weld parameters and the effect of these on weld microstructures and mechanical properties has been established. From this, it is evident that FSW generates a very complex metallurgical system.
* A preliminary FSW parameter envelope has been generated based on the outcomes of microstructural evaluation and mechanical testing. Further refinement is on-going.
* A number of weld parameters have been identified which may produce very fast welds of acceptable quality that are highly competitive to conventional fusion welding techniques, and a programme of classification compliance testing is currently being planned in collaboration with UoS, LR, CMT and TWI.
* A detailed thermo-mechanical deformation study has been undertaken, generating data not previously available for steel grade DH36, and serving as a fundamental building block for Cenaero's local microstructural numerical model.
* Key aspects of FSW of steel such as fillet welds, design and development of new tool materials and controlled heating and cooling through the use of backing strips have been identified as highly worthy of further examination.

References

Boisse, P., Altan, T., & van Luttervelt, K. (eds) (2003). *Friction and flow stress in forming and cutting*, London: Kogan Page Science.

Camilleri, D., & Gray, T. (2005). Computationally efficient welding distortion simulation techniques. *Modelling and Simulation in Materials Science and Engineering*, 13 (8), p. 1365.

Dieter, G.E., Kuhn, H.A., & Semiatin, S.L. (eds) (2003). *Handbook of Workability and Process Design*, Materials Park, OH: ASM International.

Micallef D., Camilleri D., & Mollicone P. (2013). Simplified thermo-elastoplastic numerical modelling techniques applied to friction stir welding of mild steel. *ASME 2013 Int. Mech. Eng. Congress and Exposition*.

Nowotnik, A. (2008). Flow stress value and activation energy of hot deformed Inconel superalloys. *Advances in Manufacturing Science and Technology*, 32 (4), pp. 51-62.

Roebuck, B., Lord, J.D., Brooks, M., Loveday, M.S., Sellars, C.M., & Evans, R.W. (2006). Measuring flow stress in hot axisymmetric compression tests. *Materials at High Temperatures*, 23 (2), pp. 59-83.